

# A method for classification of data with uncertainty using hypothesis testing

Shoma Yokura<sup>1</sup> and Akihisa Ichiki<sup>1\*†</sup>

Department of Applied Mathematics, Faculty of Science, Fukuoka University, 8-19-1, Nanakuma, Jonan-ku, Fukuoka City, 814-0180, Fukuoka Prefecture, Japan.

\*Corresponding author(s). E-mail(s): [ichiki@fukuoka-u.ac.jp](mailto:ichiki@fukuoka-u.ac.jp);

Contributing authors: [sd230006@cis.fukuoka-u.ac.jp](mailto:sd230006@cis.fukuoka-u.ac.jp);

†These authors contributed equally to this work.

## Abstract

Binary classification is a task that involves the classification of data into one of two distinct classes. It is widely utilized in various fields. However, conventional classifiers tend to make overconfident predictions for data that belong to overlapping regions of the two class distributions or for data outside the distributions (out-of-distribution data). Therefore, conventional classifiers should not be applied in high-risk fields where classification results can have significant consequences. In order to address this issue, it is necessary to quantify uncertainty and adopt decision-making approaches that take it into account. Many methods have been proposed for this purpose; however, implementing these methods often requires performing resampling, improving the structure or performance of models, and optimizing the thresholds of classifiers. We propose a new decision-making approach using two types of hypothesis testing. This method is capable of detecting ambiguous data that belong to the overlapping regions of two class distributions, as well as out-of-distribution data that are not included in the training data distribution. In addition, we quantify uncertainty using the empirical distribution of feature values derived from the training data obtained through the trained model. The classification threshold is determined by the  $\alpha$ -quantile and  $(1 - \alpha)$ -quantile, where the significance level  $\alpha$  is set according to each specific situation.

**Keywords:** Deep Learning, Hypothesis Testing, Histogram, Image Classification, Uncertainty

# 1 Introduction

Binary classification is a task to classify data into two different classes and has been applied in various fields. However, conventional classifiers tend to assign data to one of the classes, even for data points that fall within overlapping regions of the two class distributions or lie outside the distribution. In such cases, the classifier may make overconfident predictions, leading to an increased risk of misclassification, particularly for uncertain data. In high-risk domains, there are situations where conventional classifiers should not be applied. For example, in the medical field, ambiguous cases often arise during image diagnosis. In such scenarios, traditional classifiers lack the ability to respond with "I don't know" when faced with uncertain data (Laves et al., 2019; Ghoshal and Tucker, 2020). To address this issue, many methods have been proposed for quantifying uncertainty and improving the decision-making process.

In the field of uncertainty quantification, Bayesian inference methods are well-known. While applying Bayesian Neural Networks (BNN (Hinton and van Camp, 1993; Blundell et al., 2015)) tends to increase computational costs, recent methods have been proposed to address this issue by applying Monte Carlo Dropout (MC-Dropout (Gal and Ghahramani, 2015, 2016)), which is based on the Dropout (Srivastava et al., 2014) technique originally proposed for regularization. This approach enables uncertainty quantification while keeping computational costs lower. In the decision-making process, a method called Classification with Reject Option (Chow, 2006; El-Yaniv and Wiener, 2010) has been proposed. In this approach, if the value of the confidence function is below a pre-set threshold, the prediction is rejected. The confidence function is often defined based on the variance from MC-Dropout (Geifman and El-Yaniv, 2017, 2019) or the softmax response (Cordella et al., 1995). Additionally, the threshold is set as a parameter and requires optimization.

We propose a novel decision-making approach using two types of hypothesis tests. This method employs features obtained from a model trained on the training data. When applying this method to a binary classification problem, the distribution of each class can be approximated by the empirical distribution of the features obtained from the training data, and uncertainty can be quantified based on this empirical distribution. The threshold for classification is determined by the  $\alpha$  quantile and the  $1 - \alpha$  quantile, which are based on the significance level  $\alpha$  of the hypothesis test. Our method has the ability to detect data belonging to the overlapping region of the two class distributions as well as out-of-distribution data. Furthermore, in uncertainty quantification, there is no need for resampling or model refinement. By using hypothesis testing, the threshold is determined based on the significance level. Since this significance level is appropriately set according to the context, there is no need for optimization, which helps to reduce computational costs.

The structure of this paper is as follows: In the next section we introduce the two types of hypothesis tests. We define the test statistics and their distributions. In Section 3, we apply our method to the binary classification task of spiral pattern data. We examine whether our method captures the uncertainty. In Section 4, we apply our method to the task of binary classification of chest X-ray images as positive or negative for pneumonia. In the last section, we discuss the experimental results of Sections 3 and 4 and conclude.

## 2 Proposed method

### 2.1 Two types of hypothesis testing

Let  $x$  be a vector in  $\mathbb{R}^D$  and  $g : \mathbb{R}^D \rightarrow \mathbb{R}$  be a map. Let  $C_1$  and  $C_2$  be the classes in the binary classification problem, and let  $F_1(z)$  and  $F_2(z)$  ( $z \in \mathbb{R}$ ) be probability distributions that the feature values of the respective classes follow. For  $i = 1, 2$ , let  $H_0^i$  be the null hypothesis that the data  $x$  does not belong to  $C_i$  and  $H_1^i$  be the alternative hypothesis that  $x$  belongs to  $C_i$ . The following two types of hypothesis tests are conducted on the feature  $g(x)$ :

$$H_0^1 : g(x) \not\sim F_1, \quad H_1^1 : g(x) \sim F_1, \quad (1)$$

$$H_0^2 : g(x) \not\sim F_2, \quad H_1^2 : g(x) \sim F_2. \quad (2)$$

The hypothesis test (1) verifies whether the data  $x$  belongs to class  $C_1$ , and the hypothesis test (2) does whether it belongs to class  $C_2$ . The rejection regions of the aforementioned hypothesis tests are denoted by  $I_1$  and  $I_2$ , respectively, and the acceptance regions are defined as  $I_1^c = \mathbb{R} \setminus I_1$  and  $I_2^c = \mathbb{R} \setminus I_2$ . The two classes are deemed uncertain if both types of hypothesis tests can be rejected, i.e., if the value of the test statistic is an element of  $I_1$  and  $I_2$ . Additionally, if neither type of hypothesis test can be rejected, i.e., if the value of the test statistic is an element of  $I_1^c$  and  $I_2^c$ , then the two classes are considered uncertain as well.

### 2.2 Test statistic

In the context of our hypothesis testing, the test statistic, denoted by  $t$ , is specified as follows:

$$t = g(x), \quad (3)$$

where the map  $g$  corresponds to the discriminant function in the case of Support Vector Machine (SVM(Vapnik, 1998; Ghosh et al., 2019)). In the context of binary classification with a neural network, the map  $g$  that satisfies  $\sigma(g(x)) = 1/(1 + \exp(-g(x)))$  is selected as the test statistic. The quantity  $\sigma(-g(x))$  corresponds to the probability that  $x$  belongs to the class  $C_1$ .

### 2.3 Probability distribution of test statistic

In the context of hypothesis testing, it is imperative to ascertain the probability distributions  $F_1$  and  $F_2$  for the two classes  $C_1$  and  $C_2$ , respectively. However, the true probability distributions are not known. Assuming the utilization of supervised learning, class labels are assigned to the training data. Consequently, it becomes feasible to approximate the two probability distributions with the empirical ones.

Let  $D = \{(t_i, y_i) | t_i \in \mathbb{R}, y_i \in \{-1, 1\}, i = 1, 2, \dots, N\}$  be the set of training data. Defining  $D_1 = \{(t_n, 1) | n = 1, 2, \dots, N_1\}$  as the set consisting of data only in the class

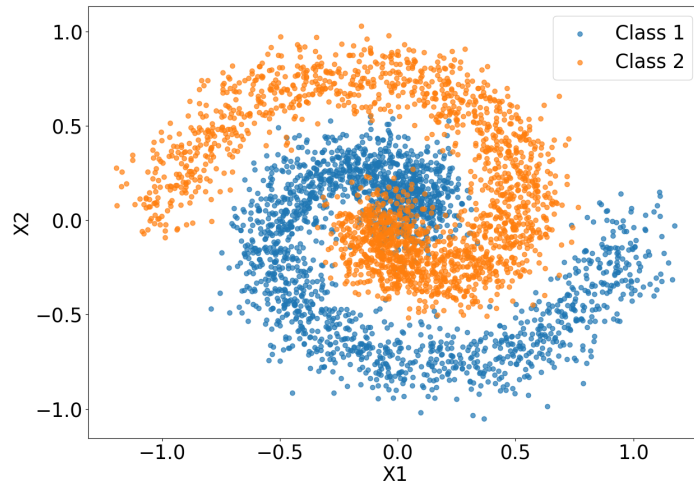


**Fig. 1** This is a dataset of spiral patterns. Each point is colored according to its correct class. Orange points are  $C_1$  and blue points are  $C_2$ .

$C_1$ , the distribution  $F_1(t)$  of  $C_1$  is approximated as follows:

$$\begin{aligned} F_1(t) &\approx \hat{F}_1(t) \\ &= \frac{1}{N_1} \sum_{n=1}^{N_1} \delta(t - t_n), \end{aligned} \quad (4)$$

where  $\delta(\cdot)$  is the Dirac delta function. The empirical distribution of  $C_2$  is also approximated as  $F_2 \approx \hat{F}_2$  in the same way as in equation (4). By approximating the true distributions with the corresponding empirical ones, it becomes possible to visualize the distributions using the histograms of the feature values. Visualization is an important key to setting the appropriate significance level for hypothesis testing.

### 3 Benchmark test

The proposed method is applied to the binary classification problem for spiral patterns, as illustrated in Figure 1. Class 1 is denoted as  $C_1$  and Class 2 as  $C_2$ . The purpose of this experiment is to visualize class regions. Therefore, all the data in Figure 1 are used as training data. The SVM (Vapnik, 1998; Ghosh et al., 2019) is utilized as the classifier for binary classification. The radial basis function (RBF) kernel  $K(x, y) = \exp(-\|x - y\|^2)$ , is employed as the kernel function of the SVM. Let  $\{x_l\}_{l=1}^L$  denote the support vector,  $\{y_l\}_{l=1}^L$  denote the label,  $\{\alpha_l \in \mathbb{R} | l = 1, 2, \dots, L\}$  and  $b \in \mathbb{R}$  be the parameters. In this case, the discriminant function is  $g(x) = \sum_{l=1}^L \alpha_l y_l K(x, x_l) + b$ , and the value of this function is used as the test statistic.

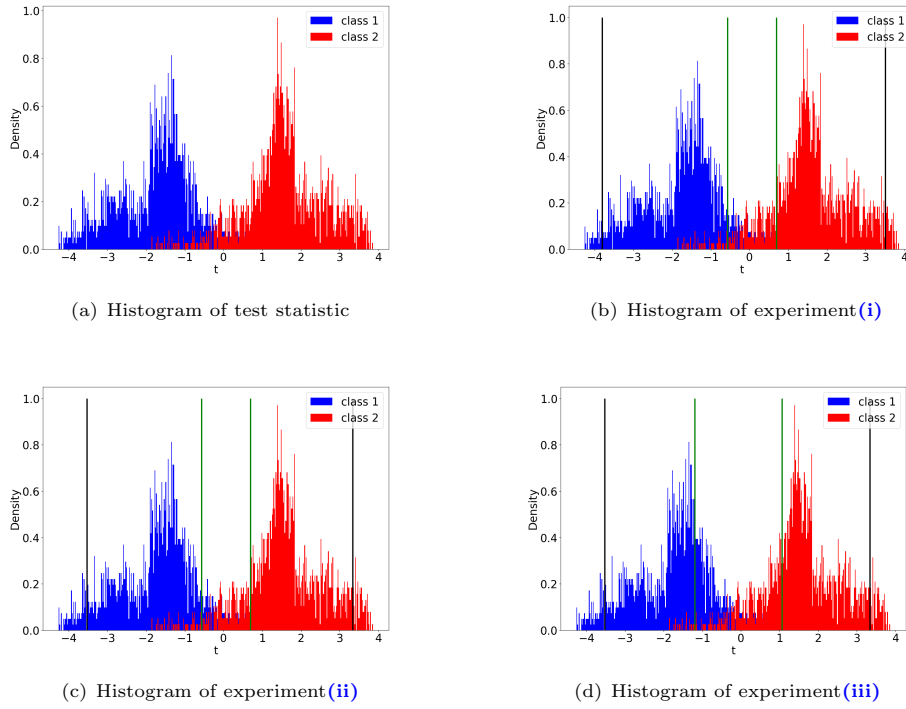


**Fig. 2** Histograms of the test statistics obtained from the training data and visualization of the histograms for each experiment.

The histogram for each class obtained from the training data is shown in Figure 2(a). Three experiments were conducted: (i), (ii), and (iii).

- (i) In Test (1), the acceptance region is defined as the interval between the 2.5% and 97.5% points, and in Test (2), the acceptance region is defined as the interval between the 2.5% and 97.5% points.
- (ii) In Test (1), the acceptance region is defined as the interval between the 5.0% and 97.5% points, and in Test (2), the acceptance region is defined as the interval between the 2.5% and 95.0% points.
- (iii) In Test (1), the acceptance region is defined as the interval between the 5.0% and 99.0% points, and in Test (2), the acceptance region is defined as the interval between the 1.0% and 95.0% points.

The histograms for experiments (i), (ii), and (iii) are shown in Figures 2(b), 2(c), and 2(d), respectively, with the intervals of uncertainty indicated between the green lines (uncertainty 1) and outside the black lines (uncertainty 2). In the context of our

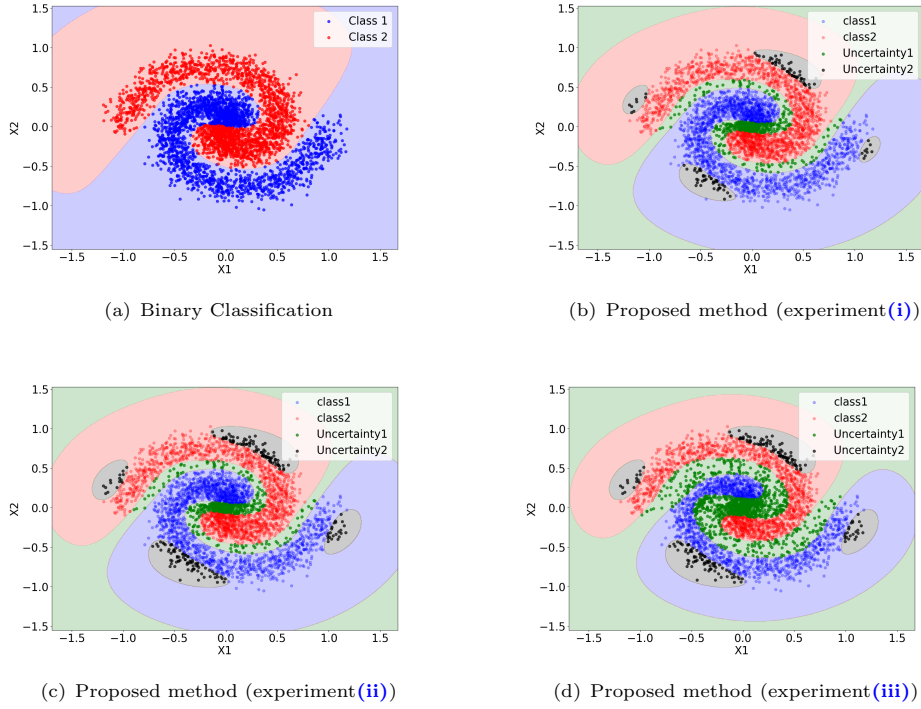


**Fig. 3** Visualization of class regions when applying the proposed method and when applying normal binary classification

two types of hypothesis testing, if one null hypothesis is rejected and the other remains unrefuted, the data is designated as  $C_1$  or  $C_2$ . To illustrate, when  $H_0^1$  is rejected but  $H_0^2$  remains valid, the data is classified as  $C_1$ . The outcomes of the binary classification are depicted in Figure 3(a). The results of experiments (i), (ii), and (iii) are shown in Figures 3(b), 3(c), and 3(d), respectively. In the case of the conventional binary classification (Figure 3(a)), the data near the discrimination boundary are classified as  $C_1$  or  $C_2$ . Conversely, the proposed method categorizes data near the discrimination boundary as uncertain data, while the remaining data are classified as  $C_1$  or  $C_2$ . A comparison of these results reveals that the proposed method effectively distinguishes between data while preserving the classification of data whose basis is ambiguous. This outcome aligns with our intuitive understanding.

## 4 Application to medical

In this section, we will apply the proposed method to the task of binary classification of pneumonia from chest X-ray images using deep learning. Many studies employ deep learning to perform binary classification for pneumonia (Tyagi et al., 2021; Joseph and Anitha, 2024; Arulananth et al., 2024; Sharma and Guleria, 2023). The models applied in these studies are unable to accurately distinguish between images that can

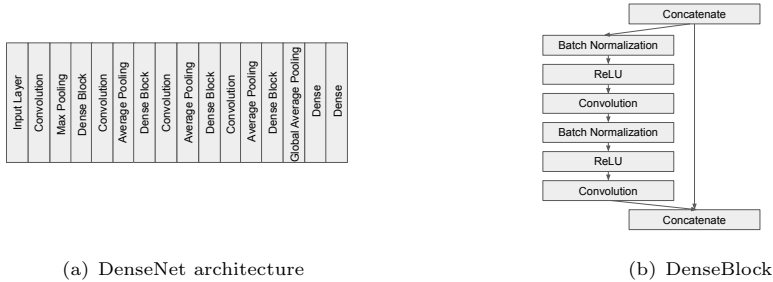


**Fig. 4** (a) shows the basic architecture of DenseNet. (b) shows the DenseBlock within DenseNet.

be managed with follow-up observation and those requiring additional intervention. As a result, even cases that could be resolved with simple follow-up may require unnecessary attention, potentially placing an excessive burden on the individuals involved in subsequent processes. Therefore, it is necessary to consider uncertainty for application in clinical settings (Leibig et al., 2017; Ghesu et al., 2021; Zou et al., 2023; Seoni et al., 2023).

## 4.1 Data preprocessing

The dataset utilized in this study is composed of chest X-ray images (Pneumonia) obtained from Kaggle (Mooney, 2017). The dataset consists of a total of 5,856 chest X-ray images, which are divided into training and test datasets. The training dataset contains 5,232 images, of which 3,883 are positive cases of pneumonia and 1,349 are negative cases. The test dataset contains 623 images, with 390 positive cases and 234 negative cases. Given the variation in image dimensions, the images are resized to a uniform size of  $256 \times 256$  pixels. Subsequently, the pixel values are normalized within the range of 0 to 1.

## 4.2 DenseNet

DenseNet (Huang et al., 2017; Anggreainy et al., 2021; M et al., 2024; Arulananth et al., 2024) is utilized as the feature extractor. The overall structure of the network is illustrated in Figure 4(a), and certain Dense Blocks contained within the network are depicted in Figure 4(b). Let  $z_l$  denote the output of the  $l$ th layer of the Dense Block. The input to layer  $l$  is the output values of the feature map of all the preceding layers:

$$z_l = H([z_0, z_1, \dots, z_{l-1}]), \quad (5)$$

where  $[z_0, z_1, \dots, z_{l-1}]$  is the concatenation of these feature maps across the respective layers, and  $H(\cdot)$  is a composite function that acts in the order of Batch Normalization (BN), Rectified Linear Unit function (ReLU), and Convolution.

### 4.3 Loss function

The number of data used in this experiment is biased (see Section 4.1). Although the training data in this experiment contains more positive images than negative images, no prior information about the test images should be assumed when employing our method in image diagnostic support. To address this issue, the loss function is weighted by the importance of the data. The sample sizes are denoted by  $N$  and  $N_1$  and  $N_2$  for the negative and positive samples, respectively. The correct label,  $y_n$ , is defined as 0 or 1. The predicted probability for the label is defined as  $\hat{y}_n$ . The loss function with importance weight, which is based on the cross-entropy method commonly used in classification problems (Shimodaira, 2000; Sugiyama et al., 2007), is given as follows:

$$\mathcal{L} = - \sum_{n=1}^N w_n \{y_n \log \hat{y}_n + (1 - y_n) \log(1 - \hat{y}_n)\},$$

where

$$w_n = \begin{cases} \frac{N_2}{N}, & \text{if } y_n = 0 \\ \frac{N_1}{N}, & \text{if } y_n = 1 \end{cases}$$

### 4.4 Experiment method

As delineated in Section 4.2, the DenseNet-121 (Arulananth et al., 2024) is employed as the feature extractor. This network is pre-trained on ImageNet, and fine-tuning is achieved through the utilization of training images. The Adam optimization method is employed for parameter tuning. The learning rate is set to  $1.0 \times 10^{-3}$ , and the Adam optimizer is used. The test statistic, denoted by  $g(x)$ , satisfies the following equation:  $\sigma(x) = 1/(1 + e^g(x))$  (see Section 2.2). The binary classification of negative/positive is performed using two types of hypothesis tests, as outlined in Section 3. However, the distinction between the types of uncertainty defined in Section 3 is not made in this section. Let  $\alpha$  denote the significance level. In this experiment, the parameter  $\alpha$  is employed to delineate the two types of hypothesis tests at a common significance level. The experiment is conducted for values of  $\alpha = 1.0\%$ ,  $2.5\%$ , and  $5.0\%$ . The performance of the experiment is evaluated using metrics such as coverage, accuracy, precision, recall, specificity, and the F1-score. Coverage is defined as the ratio of test data that produces results of the prediction, and is expressed as follows:

$$Coverage = 1 - \frac{\#(Uncertainty \ data)}{\#(ALL \ data)}.$$

The accuracy, recall, precision, specificity, and F1-score are calculated using data that was not judged to be uncertain.

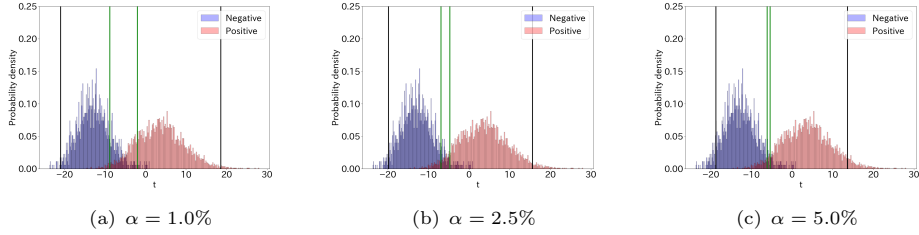


**Fig. 5** The histograms of the test statistics at significance levels  $\alpha = 1.0\%$ ,  $2.5\%$ , and  $5.0\%$  are shown. The blue histogram represents the distribution of the test statistics for negative data, while the red histogram represents the distribution of the test statistics for positive data.

**Table 1** Experimental results at significance levels  $\alpha = 1.0\%$ ,  $2.5\%$ ,  $5.0\%$

$\alpha(\%)$	coverage	Accuracy(%)	Recall(%)	Precision(%)	Specificity(%)	F1-Score
1.0	0.84	99.24	99.07	99.68	99.37	99.37
2.5	0.93	98.68	97.80	99.44	99.07	98.61
5.0	0.94	97.39	96.97	98.87	98.10	97.92

## 4.5 Result

When the significance level  $\alpha$  was set to  $1.0\%$ ,  $2.5\%$ , and  $5.0\%$ , the histograms of the test statistics corresponding to each level are shown in Figures 5(a), 5(b), and 5(c). It was observed that as the significance level increased (e.g., from  $1.0\%$  to  $2.5\%$  to  $5.0\%$ ), the range of the uncertainty interval tended to gradually narrow. The experimental results for each significance level are shown in Table 1. As the significance level increases, the coverage increases, while accuracy and other evaluation metrics tend to decrease.

## 5 Discussion and conclusions

Two experiments were conducted in sections 3 and 4 of this paper. The results of these experiments confirmed that as the uncertainty interval widens, the process classifies data into one of the two classes only when the data can be judged with higher confidence. Additionally, it was revealed that the coverage does not necessarily decrease as the significance level increases. This is because the classification thresholds are determined by the  $\alpha$  quantile and  $1 - \alpha$  quantile corresponding to the significance level  $\alpha$ . Consequently, when applying the proposed method, it is necessary to adjust the significance level to an appropriate value according to the specific context.

In this paper, we propose an approach to classification that incorporates uncertainty by introducing two types of hypothesis testing. In previous studies, the quantification of uncertainty required the use of resampled or validation data, as well as the tuning of multiple hyperparameters. In contrast, the proposed method determines thresholds using only training data, significantly reducing computational and time costs compared to conventional methods. Furthermore, as described in Section 2, the proposed approach establishes thresholds based on the significance level defined

by hypothesis testing, providing a solid theoretical foundation. Another feature of the proposed method is its ability to leverage histograms to visually capture ambiguous regions between classes while effectively detecting uncertain data. While this study focuses on applications in the medical field, the proposed method is expected to be applicable to other domains as well.

## References

- Arulananth, T.S., Prakash, S.W., Ayyasamy, R.K., Kavitha, V.P., Kuppasamy, P.G., Chinnasamy, P.: Classification of paediatric pneumonia using modified densenet-121 deep-learning model. *IEEE Access* **12**, 35716–35727 (2024) <https://doi.org/10.1109/ACCESS.2024.3371151>
- Arulananth, T., Prakash, S.W., Ayyasamy, R.K., Kavitha, e.a.: Classification of paediatric pneumonia using modified densenet-121 deep-learning model. *IEEE Access* (2024) <https://doi.org/10.1109/ACCESS.2024.3371151>
- Anggreainy, M.S., Wulandari, A., Ilyyasu, A.M.: Pneumonia detection using dense convolutional network (densenet) architecture. In: 2021 4th International Seminar on Research of Information Technology and Intelligent Systems (ISRITI), pp. 556–559 (2021). <https://doi.org/10.1109/ISRITI54043.2021.9702803>
- Blundell, C., Cornebise, J., Kavukcuoglu, K., Wierstra, D.: Weight uncertainty in neural networks. In: Proceedings of the 32nd International Conference on International Conference on Machine Learning - Volume 37. ICML'15, pp. 1613–1622. JMLR.org, Lille, France (2015). <https://doi.org/10.1145/.1772690.1772758>
- Cordella, L.P., De Stefano, C., Tortorella, F., Vento, M.: A method for improving classification reliability of multilayer perceptrons. *IEEE Transactions on Neural Networks* **6**(5), 1140–1147 (1995) <https://doi.org/10.1109/72.410358>
- Chow, C.: On optimum recognition error and reject tradeoff. *IEEE Trans. Inf. Theor.* **16**(1), 41–46 (2006) <https://doi.org/10.1109/TIT.1970.1054406>
- El-Yaniv, R., Wiener, Y.: On the foundations of noise-free selective classification. *Journal of Machine Learning Research* **11**(53), 1605–1641 (2010) <https://doi.org/10.5555/1756006.1859904>
- Ghosh, S., Dasgupta, A., Swetapadma, A.: A study on support vector machine based linear and non-linear pattern classification. In: 2019 International Conference on Intelligent Sustainable Systems (ICISS), pp. 24–28 (2019). <https://doi.org/10.1109/ISS1.2019.8908018>
- Geifman, Y., El-Yaniv, R.: Selective classification for deep neural networks. *ArXiv abs/1705.08500* (2017) <https://doi.org/10.48550/arXiv.1705.08500>
- Geifman, Y., El-Yaniv, R.: SelectiveNet: A deep neural network with an integrated

- reject option. In: Chaudhuri, K., Salakhutdinov, R. (eds.) Proceedings of the 36th International Conference on Machine Learning. Proceedings of Machine Learning Research, vol. 97, pp. 2151–2159. PMLR, Long Beach, California (2019). <https://proceedings.mlr.press/v97/geifman19a.html>
- Gal, Y., Ghahramani, Z.: Dropout as a bayesian approximation. arXiv preprint arXiv:1506.02157 (2015) <https://doi.org/10.48550/arXiv.1506.02142>
- Gal, Y., Ghahramani, Z.: Dropout as a bayesian approximation: Representing model uncertainty in deep learning. In: Balcan, M.F., Weinberger, K.Q. (eds.) Proceedings of The 33rd International Conference on Machine Learning. Proceedings of Machine Learning Research, vol. 48, pp. 1050–1059. PMLR, New York, New York, USA (2016). <https://proceedings.mlr.press/v48/gal16.html>
- Ghesu, F.C., Georgescu, B., Mansoor, A., Yoo, Y., Gibson, E., Vishwanath, R., Balachandran, A., Balter, J.M., Cao, Y., Singh, R., Singh, R., Digumarthy, S.R., Kalra, M.K., Grbic, S., Comaniciu, D.: Quantifying and leveraging predictive uncertainty for medical image assessment. *Medical image analysis* **68**, 101855 (2021) <https://doi.org/10.1016/j.media.2020.101855>
- Ghoshal, B., Tucker, A.: Estimating uncertainty and interpretability in deep learning for coronavirus (covid-19) detection. arXiv preprint arXiv:2003.10769 (2020) <https://doi.org/10.48550/arXiv.2003.10769>
- Huang, G., Liu, Z., Van Der Maaten, L., Weinberger, K.Q.: Densely connected convolutional networks. In: Proceedings of the IEEE Conference on Computer Vision and Pattern Recognition, pp. 4700–4708 (2017). <https://doi.org/10.1109/CVPR.2017.243>
- Hinton, G.E., Camp, D.: Keeping the neural networks simple by minimizing the description length of the weights. In: Proceedings of the Sixth Annual Conference on Computational Learning Theory. COLT '93, pp. 5–13. Association for Computing Machinery, New York, NY, USA (1993). <https://doi.org/10.1145/168304.168306>
- Joseph, H., Anitha, J.: Enhanced pneumonia detection through advanced ai-driven hybrid models: A comparative study of deep learning architectures. In: 2024 1st International Conference on Trends in Engineering Systems and Technologies (ICTEST), pp. 01–05 (2024). <https://doi.org/10.1109/ICTEST60614.2024.10576088>
- Leibig, C., Allken, V., Ayhan, M.S., Berens, P., Wahl, S.: Leveraging uncertainty information from deep neural networks for disease detection. *Scientific reports* **7**(1), 1–14 (2017) <https://doi.org/10.1038/s41598-017-17876-z>
- Laves, M.-H., Ihler, S., Ortmaier, T.: Uncertainty Quantification in Computer-Aided Diagnosis: Make Your Model say “I don’t know“ for Ambiguous Cases (2019). <https://openreview.net/forum?id=rJevPsX854>

- Mooney, P.: Chest X-Ray Images (Pneumonia). <https://www.kaggle.com/datasets/paultimothymooney/chest-xray-pneumonia>. Licensed under CC BY 4.0. Accessed: 2024-11-29 (2017)
- M, S., Sai, B.C., Tinnaluri, Y., Tella, T.: Accurate prediction of classification score using densenet for acute pneumonia. 2024 2nd International Conference on Intelligent Data Communication Technologies and Internet of Things (IDCIoT), 1293–1299 (2024) <https://doi.org/10.1109/IDCIoT59759.2024.10467683>
- Sharma, S., Guleria, K.: A deep learning based model for the detection of pneumonia from chest x-ray images using vgg-16 and neural networks. *Procedia Computer Science* **218**, 357–366 (2023) <https://doi.org/10.1016/j.procs.2023.01.018>. International Conference on Machine Learning and Data Engineering
- Shimodaira, H.: Improving predictive inference under covariate shift by weighting the log-likelihood function. *Journal of Statistical Planning and Inference* **90**(2), 227–244 (2000) [https://doi.org/10.1016/S0378-3758\(00\)00115-4](https://doi.org/10.1016/S0378-3758(00)00115-4)
- Srivastava, N., Hinton, G., Krizhevsky, A., Sutskever, I., Salakhutdinov, R.: Dropout: A simple way to prevent neural networks from overfitting. *Journal of Machine Learning Research* **15**(56), 1929–1958 (2014) <https://doi.org/10.5555/2627435.2670313>
- Seoni, S., Jahmunah, V., Salvi, M., Barua, P.D., Molinari, F., Acharya, U.R.: Application of uncertainty quantification to artificial intelligence in healthcare: A review of last decade (2013–2023). *Computers in Biology and Medicine*, 107441 (2023) <https://doi.org/10.1016/j.compbiomed.2023.107441>
- Sugiyama, M., Krauledat, M., Müller, K.-R.: Covariate shift adaptation by importance weighted cross validation. *Journal of Machine Learning Research* **8**(35), 985–1005 (2007) <https://doi.org/10.5555/1314498.1390324>
- Tyagi, K., Pathak, G., Nijhawan, R., Mittal, A.: Detecting pneumonia using vision transformer and comparing with other techniques. In: 2021 5th International Conference on Electronics, Communication and Aerospace Technology (ICECA), pp. 12–16 (2021). <https://doi.org/10.1109/ICECA52323.2021.9676146>. IEEE
- Vapnik, V.N.: *Statistical Learning Theory*. Wiley-Interscience, New York (1998)
- Zou, K., Chen, Z., Yuan, X., Shen, X., Wang, M., Fu, H.: A review of uncertainty estimation and its application in medical imaging. *Meta-Radiology*, 100003 (2023) <https://doi.org/10.1016/j.metrad.2023.100003>